Prepared for submission to JCAP

Extending Higgs Inflation with TeV Scale New Physics

Hong-Jian He, [a,c,d] **Zhong-Zhi Xianyu** [a,b]

[a] Institute of Modern Physics and Center for High Energy Physics, Tsinghua University, Beijing 100084, China
[b] Theoretical Particle Physics and Cosmology Group, Department of Physics, King's College London, London WC2R 2LS, UK
[c] Center for High Energy Physics, Peking University, Beijing 100871, China
[d] Kavli Institute for Theoretical Physics China, CAS, Beijing 100190, China

E-mail: hjhe@tsinghua.edu.cn, xianyuzhongzhi@gmail.com

Abstract.

Higgs inflation is among the most economical and predictive inflation models, although the original Higgs inflation requires tuning the Higgs or top mass away from its current experimental value by more than 2σ deviations, and generally gives a negligible tensor-to-scalar ratio $r \sim 10^{-3}$ (if away from the vicinity of critical point). In this work, we construct a minimal extension of Higgs inflation, by adding only two new weak-singlet particles at TeV scale, a vector-quark $\mathcal{T}$ and a real scalar $\mathcal{S}$. The presence of singlets $(\mathcal{T}, \mathcal{S})$ significantly impact the renormalization group running of the Higgs boson self-coupling. With this, our model provides a wider range of the tensor-to-scalar ratio $r = \mathcal{O}(0.1 - 10^{-3})$, consistent with the favored r values by either BICEP2 or Planck data, while keeping the successful prediction of the spectral index $n_s \simeq 0.96$. It further allows the Higgs and top masses to fully fit the collider measurements. We also discuss implications for searching the predicted TeV-scale vector-quark $\mathcal{T}$ and scalar $\mathcal{S}$ at the LHC and future high energy pp colliders.

Keywords:

Inflation, Cosmology of theories beyond the SM, Particle physics – Cosmology connection

JCAP (2014), final version [arXiv:1405.7331]

arXiv:1405.7331v3 [hep-ph] 9 Oct 2014

Contents

1 Introduction 2

2 Minimal Extension of Higgs Inflation with Two Weak-Singlets 4

3 Improved Scalar Potential and New Predictions for Higgs Inflation 8

4 Conclusions and Discussions 14

Acknowledgments 16

A Renormalization Group Equations for Higgs Inflation Analysis 16

References 18

1 Introduction

Cosmic inflation [1–5] successfully describes the evolution of the very early universe. It not only resolves problems of the standard big-bang cosmology (such as horizon problem and flatness problem), but also generates primordial fluctuations, which shape the large scale structure of the universe. The amplitudes and shapes of these fluctuations can be directly tested by the observations of CMB and large scale structure. The recent BICEP2 discovery of B-mode in the CMB polarization [6] has provided strong evidence that the gravitational waves (with a quantum origin) were created during inflation. The BICEP2 tensor-to-scalar ratio $r = 0.20^{+0.07}_{-0.05}$ [6], if confirmed, will strongly constrain viable models of inflation. With Planck normalization $(V/\epsilon)^{1/4} = 0.027 M_{\rm Pl}$ [7], it also reveals the energy scale of inflation, $\Lambda_{\rm INF} = V^{1/4} \simeq 2\times 10^{16}\,{\rm GeV}$, where $\epsilon = r/16$ is the first slow-roll parameter, and $M_{\rm Pl} \simeq 2.44\times 10^{18}\,{\rm GeV}$ is the reduced Planck mass. The current BICEP2 data have some tension with the indirect measurement of r by Planck satellite [8] if one assumes a negligible running $\alpha_s (= {\rm d}n_s/{\rm d}\ln k)$ of spectrum index n_s. Although a large α_s can reconcile both Planck and BICEP2 results, such a large running would probably ruin the slow-roll approximation. It is desirable to further verify the dust model adopted by BICEP2 and quantify other possible sources of foreground contamination such as the magnetized dust associated with radio loops [9] or the potential dust polarization effect [10] allowed by the current Planck data [8][11]. The upcoming data from Planck, Keck Array and other B-mode measurements (such as ABS, ACTPol, EBEX, POLARBEAR, Spider and SPT) are expected to further pin down the situation.

Among all the existing inflation models, the Higgs inflation [12–14] appears the most economical and predictive one since it is the only model which uses a discovered particle — the Higgs boson [15], as the inflaton. The original model of Higgs inflation makes use of the unique dimension-4 operator of the Higgs-gravity interaction, $\xi\mathcal{R}H^\dagger H$, where $\mathcal{R}$ is the Ricci scalar curvature and H is the Higgs doublet. By taking $\xi \simeq 17000$ as required by the observed strength of curvature perturbation, the model predicts at the tree-level that the spectral index $n_s \simeq 0.967$ and the tensor-to-scalar ratio $r \simeq 0.0031$, which are in agreement with Planck data [8]. When taking account of renormalization group (RG) running, the model also exhibits some tension [16] with the measured masses of the Higgs boson and top quark [15, 17, 18].

It is clear that the original Higgs inflation model with large $\xi = \mathcal{O}(10^4)$ is disfavoured by the BICEP2 data. But there are still parameter regions in this model to give a sizable r. As noticed in Refs. [16, 20, 21], when the Higgs mass reaches its "critical point", with which the Higgs self-coupling λ runs to vanishingly small value at inflation scale, a successful inflation could be achieved by only a mildly large $\xi = \mathcal{O}(10)$, while the tensor-to-scalar ratio r can be as large as $\mathcal{O}(0.1)$. A relatively small ξ also makes the Higgs inflation fully free from the potential problem of unitarity violation [14, 23, 24]. But, it is known [16, 20, 21, 25] that the critical point for Higgs mass or top-quark mass as required in this case is already outside the 2σ ranges of the collider measurements, $m_h = 125.6 \pm 0.2(\text{stat}) \pm 0.3(\text{syst})\,\text{GeV}$ [15] and $m_t = 173.39^{+1.12}_{-0.98}\,\text{GeV}$ [18] [1]. If we use the current central values of Higgs mass and top quark mass, together with the two-loop RG running, the Higgs self-coupling will turn negative around $10^{11}\,\text{GeV}$, which is far below the expected inflation scale.

But, we should keep in mind that all the analyses mentioned above are based on a strong assumption that the standard model (SM) holds all the way up to the inflation scale, and no new particle beyond the SM would exist. This is unlikely the case, since there are many motivations for new physics showing up at the TeV scale. Hence, it is intriguing to study how the presence of new particles will improve the original Higgs inflation model and provide the corresponding new discovery signatures at colliders. Some interesting attempts appeared lately [26].

In this paper, we construct a new minimal extension for the Higgs inflation, by adding two weak-singlet particles at the TeV scale, a vector-quark $\mathcal{T}$ and a real scalar $\mathcal{S}$. We

[1] The current most precise measurement on the top-quark mass is given by the world combination of the ATLAS, CMS, CDF and D0 experiments [17], $m_t = 173.34 \pm 0.27(\text{stat}) \pm 0.71(\text{syst})\,\text{GeV}$. This is based on the best fit to the mass parameter as implemented in the respective Monte Carlo (MC) code for generating the theory input, and is usually called MC top mass. It is shown [18] that this MC mass definition can be converted to a theoretically well-defined short-distance mass definition with an uncertainty of $\sim 1\,\text{GeV}$, and the resultant pole mass is, $m_t = 173.39^{+1.12}_{-0.98}\,\text{GeV}$ [18]. As a further note, the Snowmass study [19] found that the upgraded high luminosity LHC can eventually reduce the error Δm_t down to 500 MeV, and an e^+e^- lepton collider (such as the ILC) can measure Δm_t to 100 MeV level.

will demonstrate that within such a minimal setting, the model can perfectly fit both the cosmology data (including BICEP2 [6]) and the collider measurements on Higgs and top masses [15, 17, 18]. This provides an effective way to remove the tension between the original Higgs inflation model and collider data, as well as allowing a wide range of the tensor-to-scalar ratio r in light of the BICEP2 [6] and Planck data [8]. We also note that some particle phenomenology of singlet vector-quarks were studied before in very different contexts [27, 28].

2 Minimal Extension of Higgs Inflation with Two Weak-Singlets

We may naively expect that the minimal extension of the original Higgs inflation [12] would be to add only one new particle, presumably a scalar. However, as we will show below, the current experimental values of the SM Higgs and top masses lie in such a critical region that any new heavy particle interacting with the SM Higgs would strongly affect the qualitative RG-running behavior of the Higgs self-coupling. Thus, adding just one new particle would require a higher degree of fine-tuning in general [29].

To make this clear, let us inspect the one-loop β-function of Higgs self-coupling λ in the SM,

$$\beta_\lambda^{(\mathrm{SM})} = \frac{1}{(4\pi)^2}\Big\{24\lambda^2 - 6y_t^2 + \frac{3}{8}\big[2g^4 + (g^2+g'^2)^2\big] + \lambda(-9g^2 - 3g'^2 + 12y_t^2)\Big\}, \qquad (2.1)$$

where y_t is the top Yukawa coupling, and $(g,\, g')$ are gauge couplings of $SU(2)_L \otimes U(1)_Y$. Here we have neglected the small Yukawa couplings of all light SM fermions, expect that of top quark. The contributions from gauge couplings are also numerically small as compared to that of λ and y_t. Hence, the running of λ are largely determined by the two competing factors, λ and y_t, which can be further expressed in terms of Higgs mass m_h and top mass m_t through $\lambda = m_h^2/2v^2$ and $y_t = \sqrt{2}m_t/v$ at tree-level, where $v \simeq 246\,\mathrm{GeV}$ is the vacuum expectation value of the Higgs field. Due to the large top Yukawa coupling $y_t \simeq 1$, this β-function will decrease λ with the increasing energy, and finally pushes λ to zero and negative values at a scale μ_* which we call the turning point. Inputting the current experimental central values $m_h = 125.6\,\mathrm{GeV}$ and $m_t = 173.3\,\mathrm{GeV}$, and using the two-loop RG running, we find that the turning point is around $\mu_* \sim 10^{11}\,\mathrm{GeV}$. This is far below the inflation scale $\Lambda_{\mathrm{INF}} \simeq 2.3 \times 10^{16}\,\mathrm{GeV}$, as inferred from BICEP2 measurement [6]. But the location of this turning point is rather sensitive to the Higgs and top masses. For instance, if we input a smaller top mass $m_t \simeq 171\,\mathrm{GeV}$ (beyond the 2σ lower bound of m_t data [18]), the turning point μ_* will be quickly shifted to the Planck scale $M_{\mathrm{Pl}} \simeq 2.44 \times 10^{18}\,\mathrm{GeV}$. In fact, this is the main observation invoked in the recent "critical point scenario" [16, 20, 21] of Higgs inflation as mentioned in Sec. 1.

Group	Q_{3L}	t_R	b_R	$\mathcal{T}_L$	$\mathcal{T}_R$	H	$\mathcal{S}$
$SU(2)_L$	**2**	1	1	1	1	**2**	1
$U(1)_Y$	$\frac{1}{6}$	$\frac{2}{3}$	$-\frac{1}{3}$	$\frac{2}{3}$	$\frac{2}{3}$	$\frac{1}{2}$	0
$\mathbb{Z}_2$	$-$	$-$	$-$	$+$	$-$	$+$	$-$

Table 1. Quantum number assignments for the third family quarks $(t,\, b)$, the Higgs doublet, and the new fields $(\mathcal{S},\, \mathcal{T})$ under $SU(2)_L \otimes U(1)_Y \otimes \mathbb{Z}_2$. All other fields have the same assignments as in the SM and are $\mathbb{Z}_2$ even. Here we have defined, $Q_{3L} = (t,\, b)^T_L$.

When adding new particles coupled to the Higgs field, the qualitative picture is the same as before: bosons and fermions will drive λ towards positive and negative values, respectively. Thus, adding just one scalar or fermion will generally destroy the art of exquisite balancing. Hence, we are naturally led to construct a minimal viable extension of the SM Higgs inflation by adding just two new weak-singlets, a real scalar $\mathcal{S}$ and a vector-quark $\mathcal{T}$. In the following, we will demonstrate that this model can provide a successful Higgs inflation, and achieve full agreements with the current experimental data from both cosmology and colliders.

In our construction, we impose a simple $\mathbb{Z}_2$ symmetry under which $(\mathcal{S},\, \mathcal{T}_R)$ and $(t,\, b)$ are $\mathbb{Z}_2$-odd, while all other fields are $\mathbb{Z}_2$-even. In Table 1, we summarize the quantum number assignments for the third family quarks, the Higgs doublet, and the new fields $(\mathcal{T},\, \mathcal{S})$ under $SU(2)_L \otimes U(1)_Y \otimes \mathbb{Z}_2$. Here we have defined, $Q_{3L} = (t,\, b)^T_L$. All other fields have the same assignments as in the SM.

Thus, we can write down the general scalar potential for the Higgs doublet H and the real singlet $\mathcal{S}$ as follows,

$$V(H,\mathcal{S}) \;=\; -\mu_1^2 H^\dagger H - \tfrac{1}{2}\mu_2^2 \mathcal{S}^2 + \lambda_1 (H^\dagger H)^2 + \tfrac{1}{4}\lambda_2 \mathcal{S}^4 + \tfrac{1}{2}\lambda_3 \mathcal{S}^2 H^\dagger H + \kappa\, \mathcal{S}\,, \qquad (2.2)$$

where $H = (\pi^+,\, \frac{1}{\sqrt{2}}(v + h + \mathrm{i}\pi^0))$, with $v \simeq 246\,\mathrm{GeV}$ being the electroweak vacuum expectation value of the Higgs field. The quadratic term of $\mathcal{S}$ has a negative mass-term, and thus the $\mathbb{Z}_2$ symmetry is spontaneously broken by the nonzero vacuum expectation value (VEV) of $\mathcal{S}$ field, $\langle \mathcal{S} \rangle = u = \mathcal{O}(\mathrm{TeV}) \gg v$. In our construction, we have conjectured that all interactions are $\mathbb{Z}_2$ symmetric. Thus, any possible soft $\mathbb{Z}_2$ breaking term has to be noninteracting, and the last term of (2.2) gives the unique soft $\mathbb{Z}_2$ breaking term. This term lifts the degenerate vacua of $\mathcal{S}$ and avoids the domain wall problem [30] associated with the spontaneous $\mathbb{Z}_2$ breaking. Requiring the potential (2.2) to be asymptotically bounded from below, we have the tree-level conditions, $\lambda_1, \lambda_2 > 0$ and $\lambda_1 \lambda_2 > \frac{1}{4}\lambda_3^2$. Minimizing the scalar potential (2.2), we derive two extremal conditions,

$$\lambda_1 v^2 + \frac{1}{2}\lambda_3 u^2 \;=\; \mu_1^2\,, \qquad (2.3a)$$

$$\frac{1}{2}\lambda_3 v^2 + \lambda_2 u^2 + \frac{\kappa}{u} \;=\; \mu_2^2\,, \tag{2.3b}$$

In practice, the soft breaking term is small, $\kappa/(v^3, u^3) \ll 1$. For instance, besides $v \simeq 246\,\text{GeV}$ as fixed by the Fermi constant, we have $u = \mathcal{O}(\text{TeV})$ and $\kappa = \mathcal{O}(1-10\,\text{GeV})^3$. So, we can treat the κ term as a perturbation and only keep linear terms in κ. Thus, we can derive the VEVs,

$$v \;\equiv\; v_0 + \delta_v\,, \qquad u \;\equiv\; u_0 + \delta_u\,, \tag{2.4a}$$

$$v_0^2 \;=\; \frac{2(2\lambda_2\mu_1^2 - \lambda_3\mu_2^2)}{4\lambda_1\lambda_2 - \lambda_3^2}\,, \qquad u_0^2 \;=\; \frac{2(2\lambda_1\mu_2^2 - \lambda_3\mu_1^2)}{4\lambda_1\lambda_2 - \lambda_3^2}\,, \tag{2.4b}$$

$$\delta_v \;\simeq\; \frac{\lambda_3}{4\lambda_1\lambda_2 - \lambda_3^2}\frac{\kappa}{v_0 u_0}\,, \qquad \delta_u \;\simeq\; \frac{\lambda_1\kappa}{\lambda_3\mu_1^2 - 2\lambda_1\mu_2^2}\,. \tag{2.4c}$$

For our later numerical analysis of Higgs inflation in Sec. 3, we find that the small linear κ term has negligible effect on our samples in Table 2, because it does not affect the interaction terms and RG running.

From Table 1, we further construct the relevant Yukawa interactions for the $(t,\,\mathcal{T})$ sector,

$$\mathscr{L}_{t\mathcal{T}} \;=\; -y_1\bar{Q}_{3L}\tilde{H}t_R - y_2\bar{Q}_{3L}\tilde{H}\mathcal{T}_R - \frac{y_3}{\sqrt{2}}\mathcal{S}\,\bar{\mathcal{T}}_L\mathcal{T}_R - \frac{y_4}{\sqrt{2}}\mathcal{S}\,\bar{\mathcal{T}}_L t_R + \text{h.c.}\,, \tag{2.5}$$

where $\tilde{H} = i\tau_2 H^*$ is the charge-conjugate of Higgs doublet. There is also a Yukawa term for b-quark mass generation, $\bar{Q}_{3L}Hb_R$. We did not display this in (2.5) since b-quark has no mixing with $\mathcal{T}$. We note that the last term on the right-hand-side of (2.5) is not independent and it can always be absorbed by a field redefinition, $\mathcal{T}_R \to \mathcal{T}_R - (y_4/y_3)t_R$. Hence, we will drop the last term of Eq. (2.5), and only deal with the three independent couplings $(y_1,\,y_2,\,y_3)$ hereafter. It is clear that the $\mathbb{Z}_2$ symmetry singles out the $(t,\,\mathcal{T})$ sector, and disallows mixings between $(t,\,\mathcal{T})$ and the light up-type quarks in the first two families. Such Yukawa mixing terms could arise via effective dimension-5 operators, e.g., $\bar{Q}_{jL}\tilde{H}t_R\mathcal{S}/\Lambda_S$ and $\bar{Q}_{jL}\tilde{H}\mathcal{T}_R\mathcal{S}/\Lambda_S$, where the family index $j = 1, 2$ and Λ_S is the associated cutoff. This naturally explains why the mixings of the third family quarks with the first two families are much smaller than those among the first two families themselves, as indicated in the CKM matrix.

After the spontaneous symmetry breaking, the scalars $(h,\,\mathcal{S})$ form a 2×2 mass-matrix $\mathbb{M}_s^2$ and its diagonalization gives the mass-eigenvalues $(m_h^2,\,m_{\mathcal{S}}^2)$,

$$\mathbb{M}_s^2 \;=\; \begin{pmatrix} \lambda_1 v^2 & \lambda_3 vu \\ \lambda_3 vu & \lambda_2 u^2 \end{pmatrix} \;=\; U(\alpha)\begin{pmatrix} m_h^2 & 0 \\ 0 & m_{\mathcal{S}}^2 \end{pmatrix} U(\alpha)^T, \tag{2.6a}$$

$$U(\alpha) \;=\; \begin{pmatrix} \cos\alpha & \sin\alpha \\ -\sin\alpha & \cos\alpha \end{pmatrix}, \qquad \tan\alpha \;=\; \frac{\lambda_1 x^2 - \lambda_2 z_h^2}{\lambda_3 x(1+z_h^2)}\,, \tag{2.6b}$$

$$(m_h^2,\, m_{\mathcal{S}}^2) \;=\; \frac{u^2}{2}\Big\{(\lambda_1 x^2+\lambda_2) \mp \big[(\lambda_1 x^2-\lambda_2)^2+4\lambda_3^2 x^2\,\big]^{\frac{1}{2}}\Big\}, \tag{2.6c}$$

where we have defined the VEV ratio $x \equiv v/u \ll 1$ and the mass-ratio $z_h \equiv m_h/m_{\mathcal{S}}$. The orthogonal diagonalization matrix $U(\alpha)$ connects the weak-eigenbasis $(h,\, \mathcal{S})$ to the mass-eigenbasis $(\hat{h},\, \hat{\mathcal{S}})$. For convenience, we will simply use the notations $(h,\, \mathcal{S})$ for mass-eigenstates in the following, unless specified otherwise. From these, we can further resolve the quartic scalar couplings in terms of the mass-eigenvalues and mixing angle,

$$\begin{aligned}
\lambda_1 \;&=\; \frac{m_h^2\cos^2\alpha + m_S^2\sin^2\alpha}{2v^2}\,,\\
\lambda_2 \;&=\; \frac{m_h^2\sin^2\alpha + m_S^2\cos^2\alpha}{2u^2}\,,\\
\lambda_3 \;&=\; \frac{m_S^2-m_h^2}{2vu}\sin 2\alpha\,.
\end{aligned} \tag{2.7}$$

In parallel, for the fermion sector, we derive the following mass-matrix for the $(t,\, \mathcal{T})$,

$$\mathbb{M}_f \;=\; \frac{v}{\sqrt{2}}\begin{pmatrix} y_1 & y_2 \\ 0 & y_3 x^{-1}\end{pmatrix}, \tag{2.8}$$

Then, we can diagonalize the symmetric matrix $\mathbb{M}_f\mathbb{M}_f^\dagger$ by the left-handed rotation $U(\theta)$ from $(t,\, \mathcal{T})_L^T$ into the mass-eigenstates $(\hat{t},\, \hat{\mathcal{T}})_L^T$, i.e., $(t,\, \mathcal{T})_L^T = U(\theta)(\hat{t},\, \hat{\mathcal{T}})_L^T$. Hence, we have

$$\mathbb{M}_f\mathbb{M}_f^\dagger = U(\theta)\begin{pmatrix} m_t^2 & 0 \\ 0 & m_{\mathcal{T}}^2\end{pmatrix}U(\theta)^\dagger\,, \tag{2.9a}$$

$$U(\theta) = \begin{pmatrix} \cos\theta & \sin\theta \\ -\sin\theta & \cos\theta\end{pmatrix}, \qquad \tan\theta \;=\; \frac{x^2(y_1^2+y_2^2)-z_t^2y_3^2}{x(1+z_t^2)y_2y_3}\,, \tag{2.9b}$$

$$(m_t^2,\, m_{\mathcal{T}}^2) = \frac{u^2}{4}\left[x^2(y_1^2+y_2^2)+y_3^2\right]\left\{1 \mp \left[1-\frac{4x^2y_2^2y_3^2}{[x^2(y_1^2+y_2^2)+y_3^2]^2}\right]^{\frac{1}{2}}\right\}, \tag{2.9c}$$

where we have defined the mass ratio $z_t \equiv m_t/m_{\mathcal{T}} \ll 1$. For convenience, we will simply denote the mass-eigenstates by the notations $(t,\, \mathcal{T})$ in the following, unless specified otherwise. With these, we can resolve the Yukawa couplings $(y_1,\, y_2,\, y_3)$ as functions of the quark mass-eigenvalues and the left-handed mixing angle,

$$\begin{aligned}
y_1 \;&=\; \frac{\sqrt{2}\,z_t}{v\left(z_t^2\sin^2\theta+\cos^2\theta\right)^{\frac{1}{2}}}\,,\\
y_2 \;&=\; \frac{(1-z_t^2)\sin 2\theta}{\sqrt{2}\,v\left(z_t^2\sin^2\theta+\cos^2\theta\right)^{\frac{1}{2}}}\,,\\
y_3 \;&=\; \frac{\sqrt{2}\,m_{\mathcal{T}}}{u}\left(z_t^2\sin^2\theta+\cos^2\theta\right)^{\frac{1}{2}}.
\end{aligned} \tag{2.10}$$

For our construction, we include the unique dimension-4 operator as in the original Higgs inflation,

$$\Delta\mathscr{L}_{\rm NMC} \;=\; \sqrt{-g}\,\xi\,\mathcal{R}H^\dagger H\,, \tag{2.11}$$

where ξ is the dimensionless non-minimal coupling[2] between the Ricci scalar-curvature $\mathcal{R}$ and the Higgs doublet H. In principle, there is another nonminimal term, $\xi_s\mathcal{R}S^2$, for the new singlet scalar S. We do not add it here because it is irrelevant to our present study. The new interactions generated by the non-minimal term $\mathcal{R}H^\dagger H$ were extensively studied in Ref. [23].

3 Improved Scalar Potential and New Predictions for Higgs Inflation

In this section, we systematically study the scalar potential by including the radiative corrections. With this, we can derive predictions on the inflationary observables, and compare them with the cosmology measurements including Planck [8] and BICEP2 [6]. We will identify the parameter space of our minimal extension, which can fit well with the favored tensor-to-scalar ratio by the BICEP2 or Planck, as well as the collider data on Higgs and top masses.

The scalar sector of the model consists of a Higgs doublet H and a real singlet $\mathcal{S}$. At the inflation scale, the scalar potential is a function of the module $|H|$, where the four components of H appear in the same manner. Without losing generality, we can choose $|H| = \frac{1}{\sqrt{2}}h$ for simplicity [31]. We first set $\mathcal{S} = 0$ for the inflation analysis, and the effect of nonzero $\mathcal{S}$ will be readily included later (cf. Fig. 3). With this setup, the scalar potential (2.2) depends only on the Higgs field h, which is identified as the inflaton.

Due to the presence of nonminimal coupling term $\xi RH^\dagger H$ in (2.11), the equation of motion for the spacetime metric $g^{(J)}_{\mu\nu}$ differs from the Einstein equation of general relativity. This is conventionally called the Jordan frame, as marked by the superscript (J) of the metric. To analyze the inflation based on the standard slow-roll formulation, we will make the field-redefinition, $g^{(J)}_{\mu\nu} = \Omega^2 g^{(E)}_{\mu\nu}$, where $\Omega^2 = 1 + \xi h^2/M_{\rm Pl}^2$. The metric $g^{(E)}_{\mu\nu}$ defines the Einstein frame and takes the standard form of Friedmann-Robertson-Walker. After this transformation to Einstein frame, the kinetic term and the potential for h becomes,

$$\mathscr{L}_h \;=\; \sqrt{-g^{(E)}}\left[\frac{\Omega^2+6\xi^2h^2/M_{\rm Pl}^2}{2\Omega^4}(\partial_\mu h)^2 - \frac{\lambda h^4}{4\Omega^4}\right], \tag{3.1}$$

where we have ignored the VEV v of Higgs field since it is negligible during inflation. We further make a field redefinition $\chi = \chi(h)$ such that,

$$\frac{{\rm d}\chi}{{\rm d}h} \;=\; \frac{\left(\Omega^2 + 6\xi^2h^2/M_{\rm Pl}^2\right)^{\frac{1}{2}}}{\Omega^2}\,. \tag{3.2}$$

[2] An alternative construction of Higgs inflation with Higgs boson minimally coupled to gravity is recently given in Ref. [22], where Einstein general relativity exhibits asymptotic safety in the ultraviolet region.

Thus, the χ field is canonically normalized in Einstein frame.

After including radiative corrections, the Higgs potential V can be compactly summarized as follows,

$$V \;=\; \frac{\lambda(\mu)\, h^4}{\left[1+\xi(\mu)h^2/M_{\rm Pl}^2\right]^2}\,, \tag{3.3}$$

where $\lambda(\mu)$ and $\xi(\mu)$ are running couplings, which are inferred by solving the renormalization group equations. As argued in [33], the beta functions for running couplings should be gauge-invariant and do not contain the anomalous dimension of Higgs field h.[3] The full set of beta functions for our analysis is presented in Appendix A. Here we only highlight the difference of the beta functions in our model from that of the SM.

The most important differences come from the new scalar $\mathcal{S}$ and new vector-quark $\mathcal{T}$. This not only introduces new couplings $\lambda_{2,3}$ and $y_{2,3}$, but also modifies the β-functions of all relevant SM couplings, including the Higgs self-coupling λ_1 and the top-Yukawa coupling y_1, as well as the three gauge couplings (g_3, g, g'). Besides, the nonminimal coupling ξ also modifies β-functions through its correction to the Higgs field in the loop. This means that all the loop-lines of Higgs field h should be multiplied by the factor s,

$$s(h) \;=\; \frac{\Omega^2(h)}{\Omega^2(h)+6\xi^2h^2/M_{\rm Pl}^2}\,. \tag{3.4}$$

The net effect of this modification is to insert the proper s-factors in the corresponding terms in β-functions. The SM β-functions and anomalous dimension with appropriate s-insertion were given in Refs. [16, 32].

At this stage, there is a potential ambiguity in choosing the renormalization scale μ [16, 33]. In the Einstein frame approach (denoted as prescription-I in the literature), the optimal choice is $\mu = h/\Omega(h)$, while in the Jordan frame approach (known as prescription-II in literature) the renormalization scale is chosen to be $\mu = h$. These two choices may be essentially different and could be regarded as the low energy remnants of different UV completions. Some recent studies attempted to reconcile these apparent differences, which suggests the quantum equivalence of the two frames [34]. We keep open-minded on this issue. For the current study, we will use the prescription-I [33], i.e., we work in Einstein frame and set the renormalization scale $\mu = h/\Omega(h)$. We also note that in a more sophisticated study, one could write $\mu = \kappa h/\Omega(h)$ and adjust $\kappa \sim \mathcal{O}(1)$ to minimize the loop-corrections to the effective potential [16]. For simplicity, we will follow Ref. [16] and set $\kappa = 1$ in the current numerical analysis. When the radiative correction is dominated by top-loop, it may be natural to choose the renormalization scale $\mu = \kappa h/\Omega(h)$ with $\kappa = y_t/\sqrt{2}$ instead. We

[3] We also note that the effect of the Higgs anomalous dimension is generally negligible and does not cause any visible effect in our numerical analysis.

Sample	u	$m_{\mathcal{S}}$	$m_{\mathcal{T}}$	α	θ	ξ
A	7 TeV	3.08 TeV	3.08 TeV	1.8×10^{-2}	1.33682×10^{-2}	7.53035
B	4 TeV	1.34 TeV	1.34 TeV	4.0×10^{-2}	3.00017×10^{-2}	10.464
C	4 TeV	1.288 TeV	1.288 TeV	4.0×10^{-2}	2.9898×10^{-2}	20.88
D	4 TeV	1.6 TeV	1.6 TeV	3×10^{-2}	2×10^{-2}	2670

Table 2. Four samples (A, B, C, D) of our parameter set, which lead to successful Higgs inflation.

note that ignoring such a factor κ could cause an uncertainty in the choice of μ and thus the numerics, though it is expected to be generally small. For illustration, let us take Sample-A in Table 2 as an example, and check how it may change by setting $\kappa = y_t/\sqrt{2}$. After a systematical analysis, we obtain the following new Sample-A$'$,

$$(u,\, m_{\mathcal{S}},\, m_{\mathcal{T}}) = (7,\, 2.87,\, 2.87)\,\text{TeV}, \quad (\alpha,\, \theta) = (1.8,\, 1.319375)\times10^{-2}, \quad \xi = 7.815\,. \tag{3.5}$$

This is to be compared with the original Sample-A in Table 2 under $\kappa = 1$. From this comparison, we see that the values of u and α in Sample-A$'$ remain the same as in Sample-A, while the values of $(\theta,\, \xi)$ change by about $(1-4)\%$, and the masses of $(\mathcal{S},\, \mathcal{T})$ by about 7%. Such small changes have little effect on the phenomenology, and our main conclusions remain the same.

Given these new ingredients, we are ready to analyze the renormalization group running for couplings and fields. We will use the full set of β-functions above the threshold of heavy particles, and the SM β-functions below the threshold. To link these different regions, we integrate out $\mathcal{S}$ at $m_{\mathcal{S}}$ and $\mathcal{T}$ at $m_{\mathcal{T}}$, by inserting their equations of motion into the Lagrangian. This will impose the matching condition $\lambda_1 = \lambda + \lambda_3^2/(4\lambda_2)$ for the scalar threshold $\mu = m_{\mathcal{S}}$, and $y_1 = y_t$ for the fermion threshold $\mu = m_{\mathcal{T}}$, where λ and y_t are the Higgs self-coupling and top-Yukawa coupling of the SM, respectively. In addition, we also use the matching condition at $\mu = m_t$ as described in [35]. For the nonminimal coupling ξ, one may set its initial value at some high scale. As shown in Table 2, our Samples (A, B, C) have $\xi = \mathcal{O}(1-20)$ which respects perturbative unitarity [23]. So it is fine to set the initial value of ξ at the Planck scale $M_{\rm Pl}$. For the Sample-D with $\xi = \mathcal{O}(10^3)$, we set the initial value of ξ at $\mu = M_{\rm Pl}/\xi$.

For numerical analysis, we input the Higgs mass and top mass to be about their current experimental central values, $m_h = 125.6\,\text{GeV}$ [15] and $m_t = 173.3\,\text{GeV}$ [17]. In Table 2, we have constructed four representative samples (A, B, C, D) for the model-parameters. As will be demonstrated below, all the four samples lead to successful Higgs inflation. In our analysis, we input both top and Higgs masses by their experimental central values [15, 17] without fine-

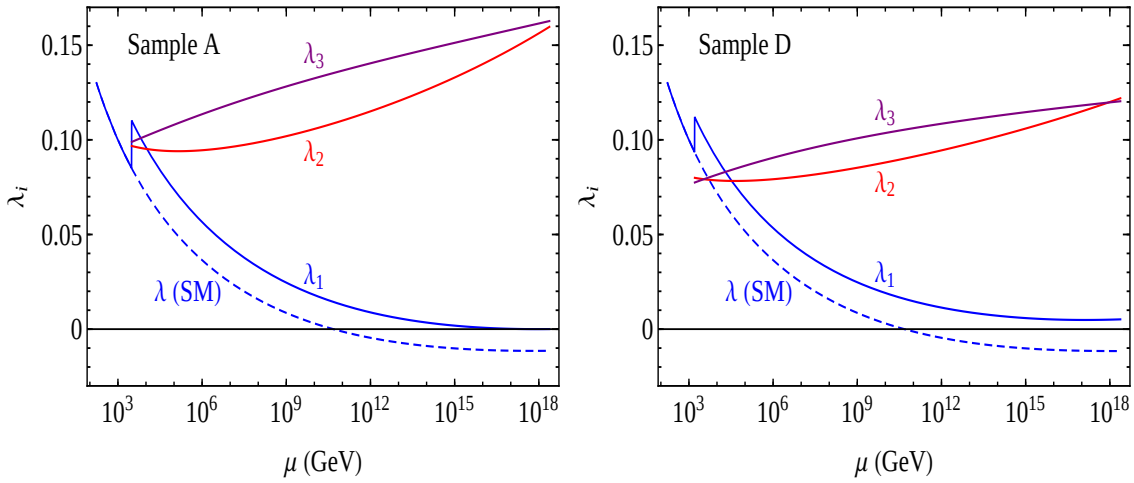

Figure 1. Running scalar couplings $(\lambda_1, \lambda_2, \lambda_3)$ as functions of the energy scale μ, from bottom to top. The Sample-A and Sample-D, as defined in Table 2, are used for the left and right plots, respectively. For comparison, we also depict the running of the SM Higgs coupling $\lambda\,(\mathrm{SM})$ in each plot by the blue dashed curve.

tuning. There are some remaining tunings only for the two theory parameters, the mixing angle θ and the nonminimal coupling ξ in the critical point scenario, corresponding to the Sample-(A, B, C); while no tuning is needed for the large-ξ scenario in our Sample-D. In each sample, for simplicity we choose equal masses for the two singlets $(\mathcal{S}, \mathcal{T})$ at the TeV scale, while in practice they are allowed to have different masses when needed. In Fig. 1, we plot the three running couplings $(\lambda_1, \lambda_2, \lambda_3)$ of the scalar sector for Sample-A and Sample-D. For comparison, we further plot the SM Higgs self-coupling λ with two-loop running, shown by the blue dashed curve in each plot of Fig. 1. As mentioned in Sec. 1, the SM Higgs self-coupling becomes negative around 10^{11} GeV, which is far below the inflation scale $\Lambda_{\rm INF} = \mathcal{O}(10^{16})$ GeV. But, our Fig. 1 demonstrates that, after including the two new particles $(\mathcal{S}, \mathcal{T})$ at TeV scale, the Higgs coupling, now called λ_1, is lifted up at the mass-threshold $\mu = m_{\mathcal{S}}$, and reaches its minimum of $\mathcal{O}(10^{-6})$ around the Planck scale $M_{\rm Pl}$. Such a small λ_1 can generate a rather flat scalar potential, and thus leads to successful inflation. In addition, we also plot the quartic scalar couplings (λ_2, λ_3) in Fig. 1, to make sure that all the scalar couplings are consistent with the stability and perturbativity. In our analysis, we have used the RG equations up to two-loop for the SM sector, and one-loop for the new physics sector (cf. Appendix A).

Given the running scalar couplings in Fig. 1, we can compute the scalar potential (3.3). This is shown by the solid curves in Fig. 2, for Sample-A and Sample-D. It is clear from these two plots that the scalar potential along h direction displays a nearly flat shape, which also has the proper height to create the observed amplitude of curvature perturbation as we will

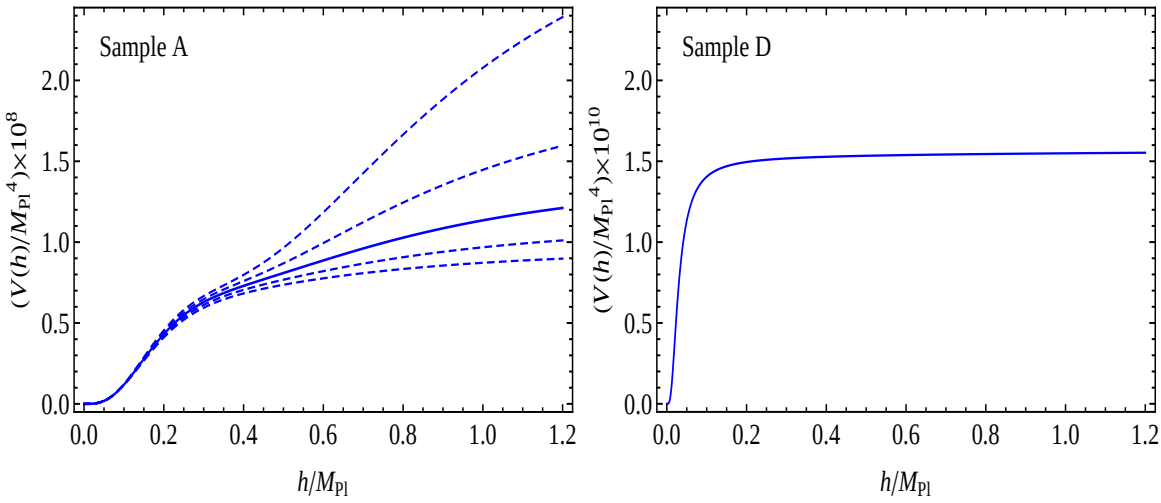

Figure 2. Scalar potential $V(h,\mathcal{S})$ in the h direction. The left plot depicts Sample-A. From bottom to top, the five curves correspond to the nonminimal coupling $\xi = \xi_0 + \Delta\xi$ with $\Delta\xi = 2,\, 1,\, 0,\, -1,\, -2$, respectively, where ξ_0 and all other parameters are taken from Sample-A of Table 2. The solid curve in the middle describes the potential with a successful Higgs inflation. For comparison, the right plot displays Sample-D with a large ξ from Table 2.

show below. To make sure this inflation potential is stable against perturbation along the $\mathcal{S}$-direction, we plot in Fig. 3 the scalar potential $V(h,\mathcal{S})$ by including nonzero $\mathcal{S}$ field, for Sample-A (left panel) and Sample-D (right panel). This plot shows that the inflation occurs along the bottom of the potential valley with $\mathcal{S} = 0$, which justifies our early setup of $\mathcal{S} = 0$ in the analysis. Here we do not include the wave function renormalization of $\mathcal{S}$ field since it is only a tiny correction and irrelevant to our calculation of inflation variables. Because the other scalar couplings $(\lambda_2,\, \lambda_3)$ remain positive and perturbative during the whole process of inflation, it is evident that the inflation path along h-direction is stable, as clearly shown in Fig. 3. The same conclusion can be drawn for Sample-(B, C), where the shape of the scalar potential is nearly the same as that of Sample-A.

To make predictions for Higgs inflation, we compute the first two slow-roll parameters ϵ and η,

$$\epsilon = \frac{M_{\rm Pl}^2}{2}\frac{V_\chi'^2}{V^2} = \frac{M_{\rm Pl}^2}{2}\left(\frac{{\rm d}h}{{\rm d}\chi}\right)^2\frac{V_h'^2}{V^2}\,, \tag{3.6a}$$

$$\eta = M_{\rm Pl}^2\frac{V_\chi''}{V} = \frac{M_{\rm Pl}^2}{V}\frac{{\rm d}h}{{\rm d}\chi}\frac{\rm d}{{\rm d}h}\left(\frac{{\rm d}h}{{\rm d}\chi}V_h'\right). \tag{3.6b}$$

The inflation ends whenever $\epsilon \simeq 1$ or $|\eta| \simeq 1$ (corresponding to $h = h_{\rm end}$), before which the universe experiences a period of nearly exponential expansion. The total amount of inflation can be quantified by the number of e-foldings N_e, which can be derived from the scalar

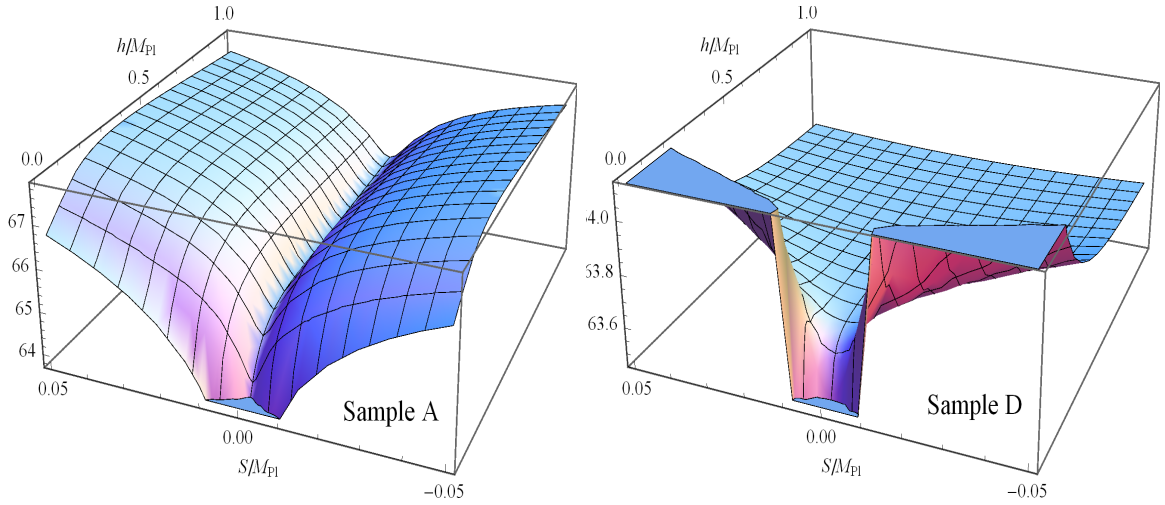

Figure 3. Scalar potential $V(h, \mathcal{S})$ as a function of fields h and $\mathcal{S}$ for Sample-A (left plot) and Sample-D (right plot). For the vertical axis in each plot, we depict the potential $V(h, \mathcal{S})$ in terms of $\log_{10}(V/\text{GeV}^4)$. All inputs are taken from Table 2.

potential,

$$N_e \;=\; \frac{1}{M_{\rm Pl}^2}\int_{h_{\rm end}}^{h_0} \mathrm{d}h\, \left(\frac{\mathrm{d}\chi}{\mathrm{d}h}\right)^2 \frac{V}{V_h'}\,. \tag{3.7}$$

The required value of N_e for observable inflation depends on the process of reheating. An analysis of reheating in Higgs inflation gives roughly $N_e \simeq 59$ [36]. Then, we can evaluate the slow-roll parameters at the beginning of these 59 folds of inflation, namely, at $h = h_0$, to get the predictions for the spectral index $n_s = 1 - 6\epsilon + 2\eta$ and the tensor-to-scalar ratio $r = 16\,\epsilon$. Furthermore, we need to make sure that the observed amplitude of curvature perturbation $V/\epsilon \simeq (0.027 M_{\rm Pl})^4$ [7] is appropriately produced.

Next, we take the four sets of sample parameters in Table 2 to compute these observables. For Sample-A, we derive the amplitude of curvature perturbation $(V/\epsilon)^{1/4} \simeq 0.027 M_{\rm Pl}$ at $h_0 \simeq 0.866 M_{\rm Pl}$. For the spectral index and the tensor-to-scalar ratio, we deduce

$$(n_s,\, r) \;\simeq\; (0.960,\, 0.186), \qquad \text{(Sample-A)}. \tag{3.8}$$

Accordingly, for Sample-B, we compute the amplitude of curvature perturbation $(V/\epsilon)^{1/4} \simeq 0.028 M_{\rm Pl}$ at $h_0 \simeq 0.819 M_{\rm Pl}$. We further derive spectral index and the tensor-to-scalar ratio,

$$(n_s,\, r) \;\simeq\; (0.958,\, 0.091), \qquad \text{(Sample-B)}. \tag{3.9}$$

For Sample-C, we infer $(V/\epsilon)^{1/4} \simeq 0.028 M_{\rm Pl}$ at $h_0 \simeq 0.731 M_{\rm Pl}$, and

$$(n_s,\, r) \;\simeq\; (0.955,\, 0.028), \qquad \text{(Sample-C)}. \tag{3.10}$$

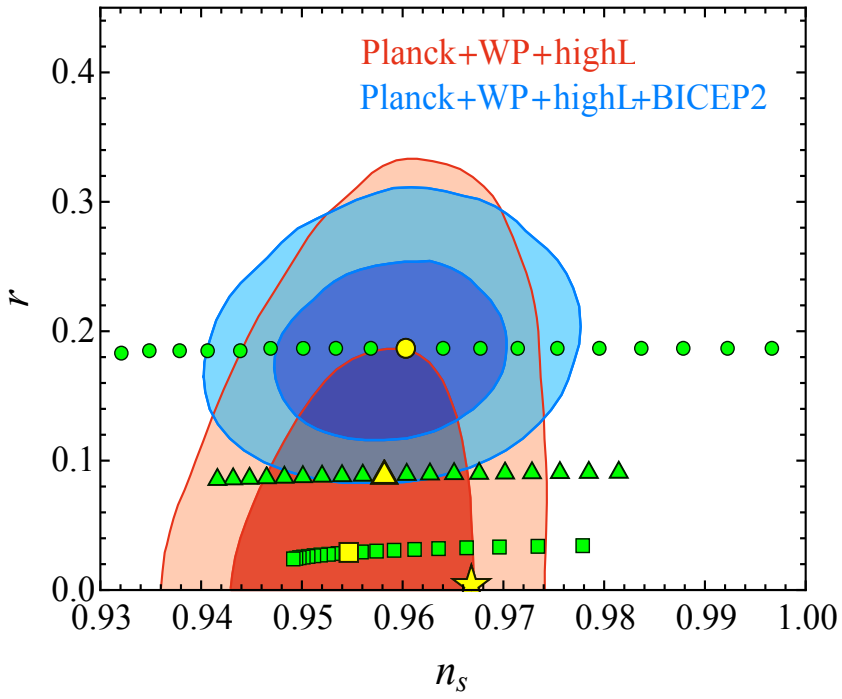

Figure 4. Sample predictions of our model for the spectral index n_s and tensor-to-scalar ratio r. The yellow (round, triangular, square, star) dot corresponds to Sample-(A, B, C, D) in Table 2. The green (round, triangular, square) dots depict the predictions of varying the nonminimal coupling ξ within $(\pm 0.0005, \pm 0.002, \pm 0.05)$ for Sample-(A, B, C), respectively. The shaded regions are observed limits at 68% C.L. and 95% C.L., taken from Fig. 13 of Ref. [6], where the measurement was made for $k = 0.002\,\mathrm{Mpc}^{-1}$.

For Sample-D, we deduce $(V/\epsilon)^{1/4} \simeq 0.028 M_{\rm Pl}$ at $h_0 \simeq 0.178 M_{\rm Pl}$, and

$$(n_s,\, r) \;\simeq\; (0.967,\, 0.005), \qquad \text{(Sample-D)}. \tag{3.11}$$

We present these predictions in Fig. 4, where the results of Sample-(A, B, C, D) are denoted by the yellow (round, triangular, square, star) dots, respectively. In the same figure, we also plot the predicted values of (n_s, r) by varying the nonminimal coupling ξ up to $\Delta\xi_{\rm max} = (\pm 0.0005, \pm 0.002, \pm 0.05)$ from the ξ values of Sample-(A, B, C) with a step equal to $0.1\Delta\xi_{\rm max}$, which are marked by green (round, triangular, square) dots for Sample-(A, B, C). It is clear from Fig. 4 that our model can successfully produce a period of inflation in the early universe. For instance, the predicted observables of Sample-(A, B) agree with the (combined) BICEP2 data [6], while the Sample-(B, C, D) have good fit with the Planck+WMAP+highL data [8].

4 Conclusions and Discussions

Higgs inflation is among the most economical and predictive inflation models on the market, although it has tension with the collider measurements of Higgs and top quark masses. In this

work, we constructed a minimal extension of the original Higgs inflation [12–14][16, 20, 21] by adding only two weak-singlet particles at TeV scale, a real scalar $\mathcal{S}$ and a vector-quark $\mathcal{T}$. In Sec. 2, we first explained why we need to include two new weak-singlets instead of one for constructing a minimal extension of the Higgs inflation. Then, we presented our model in Table 1 and Eqs. (2.2),(2.5),(2.11). From these, we derived the mass-spectra, mixing angles and couplings for both the scalar sector and the quark sector. In Sec. 3, we demonstrated that this minimal extension leads to successful Higgs inflation, consistent with the observations of BICEP2 and/or Planck, as well as the collider measurements on top and Higgs masses. In particular, we explicitly constructed representative Samples $(\mathrm{A}, \mathrm{B}, \mathrm{C}, \mathrm{D})$ as in Table 2, and presented their running scalar couplings and the shape of scalar potentials in Figs. 1-3. We further derived the predicted spectral index n_s and tensor-to-scalar ratio r in Eqs. (3.8)-(3.11). In Fig. 4, we made explicit comparison of our sample predictions of (n_s, r) with the measurements from BICEP2 [6] and Planck [8].

Some discussions are in order. A nice feature is that the present model does not finely tune the top and Higgs masses, and thus provides a better realization than the previous models of Higgs inflation [20, 21]. We note that for realizing $r = \mathcal{O}(0.1)$ in Sample-(A, B), there is some remaining tuning on the two theory parameters (the $t - \mathcal{T}$ mixing angle θ and the nonminimal coupling ξ). This is expected since the flatness of the scalar potential during inflation is achieved almost solely by the renormalization group running of scalar coupling, and thus is rather sensitive to the choice of initial conditions. But, instead of treating the fine-tuning as a problem, we may consider it as a nontrivial constraint on the model from cosmology data, and this constraint can be directly tested at the LHC and future collider experiments. For instance, the mixing between Higgs boson h and the heavy scalar $\mathcal{S}$, as well as the mixing between top quark t and heavy vector-quark $\mathcal{T}$, will modify both the production rate and the decay width of the Higgs boson $h\,(125\,\mathrm{GeV})$ at the LHC. Our analysis shows that such mixings are fairly small, around the $\mathcal{O}(10^{-2})$, and are thus fully consistent with the current LHC data so far. Since the vector-quark $\mathcal{T}$ joins QCD interactions and has mass around $1-3\,\mathrm{TeV}$, we expect it can be directly produced at the upcoming LHC $(14\,\mathrm{TeV})$ runs by gluon fusions $gg \to \mathcal{T}\overline{\mathcal{T}}$, and it mainly decays via $\mathcal{T} \to Wb$ due to the $t - \mathcal{T}$ mixing. The LHC $(14\,\mathrm{TeV})$ runs could produce the heavy scalar $\mathcal{S}$ via gluon fusion channel $gg \to \mathcal{S}$ with the subsequent decays[4] $\mathcal{S} \to WW, ZZ, hh$, which may be detected via $WW \to 2\ell 2\nu$, $ZZ \to 4\ell$, and $hh \to (WW^*)(b\bar{b}) \to (2\ell 2\nu)(b\bar{b})$, or $hh \to (\gamma\gamma)(b\bar{b})$, etc. The future high energy circular pp colliders $(50 - 100\,\mathrm{TeV})$ [38] should have much better chance to discover such TeV-scale heavy singlets $\mathcal{T}$ and $\mathcal{S}$.

[4]The production and decays of an extra heavier neutral scalar (which mixes with the observed 125 GeV Higgs particle h) was studied before for the LHC in different model contexts [37].

In our analysis, we have chosen the renormalization scale in the Einstein frame according to prescription-I of [33]. One may also consider the alternative scenario in Jordan frame, which would correspond to the chaotic inflation with quadratic potential [20]. In addition, it is useful to explore more systematically the full viable parameter space of this model, which may have reduced tuning. This will also give wider ranges of the couplings and masses of $(\mathcal{T}, \mathcal{S})$, which are useful for collider searches of such TeV scale vector-quark and neutral scalar. Finally, we may also consider embedding of our minimal extension into a SUSY framework.

Acknowledgements

We thank John R. Ellis, Yuta Hamada, Josh Ruderman, and Alexander Spencer-Smith for useful discussions on this subject. We also thank Michelangelo Mangano and Michael E. Peskin for discussing the top mass measurements. This work was supported by National NSF of China (under grants 11275101, 11135003) and National Basic Research Program (under grant 2010CB833000).

A Renormalization Group Equations for Higgs Inflation Analysis

In this appendix, we summarize the renormalization group equations which we have used to solve the running couplings. For the present model, we have three SM gauge couplings $(g_s,\, g,\, g')$ for the SM gauge group $SU(3)_c \otimes SU(2)_L \otimes U(1)_Y$, three scalar couplings $(\lambda_1,\, \lambda_2,\, \lambda_3)$ for the Higgs potential, three Yukawa coupling $(y_1,\, y_2,\, y_3)$, and a nonminimal coupling ξ. They obey the following renormalization group equations,

$$\frac{\mathrm{d}X}{\mathrm{d}\ln\mu} \;=\; \beta(g_i,\, \lambda_i,\, y_i,\, \xi)\,, \tag{A.1}$$

where X represents any coupling listed above. In the following, we will present all the relevant β functions needed for computing the scalar potential.

We first summarize the β functions in the SM up to two-loop order with appropriate s-insertion [16, 32], as well as the one-loop β function of the nonminimal-coupling ξ,

$$\beta_{g_s} = \frac{g_s^3}{(4\pi)^2}\Big(-7\Big) + \frac{g_s^3}{(4\pi)^4}\Big(\frac{11}{6}g'^2 + \frac{9}{2}g^2 - 26g_s^2 - 2sy_1^2\Big), \tag{A.2a}$$

$$\beta_{g} = \frac{g^3}{(4\pi)^2}\Big(-\frac{39-s}{12}\Big) + \frac{g^3}{(4\pi)^4}\Big(\frac{3}{2}g'^2 + \frac{35}{6}g^2 + 12g_s^2 - \frac{3}{2}sy_1^2\Big), \tag{A.2b}$$

$$\beta_{g'} = \frac{g'^3}{(4\pi)^2}\Big(\frac{81+s}{12}\Big) + \frac{g'^3}{(4\pi)^4}\Big(\frac{199}{18}g'^2 + \frac{9}{2}g^2 + \frac{44}{3}g_s^2 - \frac{17}{6}sy_1^2\Big), \tag{A.2c}$$

$$\beta_{\lambda_1} = \frac{1}{(4\pi)^2}\Big(6(1+3s^2)\lambda_1^2 - 6y_1^4 + \frac{3}{8}\big(2g^4 + (g^2+g'^2)^2\big) + \lambda_1(-9g^2 - 3g'^2 + 12y_1^2)\Big)$$
$$+ \frac{1}{(4\pi)^4}\Big[\frac{1}{48}\Big((912+3s)g^6 - (290-s)g^4g'^2 - (560-s)g^2g'^4 - (380-s)g'^6\Big)$$
$$+ (38-8s)y_1^6 - y_1^4\Big(\frac{8}{3}g'^2 + 32g_s^2 + (12-117s+108s^2)\lambda_1\Big)$$
$$+ \lambda_1\Big(-\frac{1}{8}(181+54s-162s^2)g^4 + \frac{1}{4}(3-18s+54s^2)g^2g'^2 + \frac{1}{24}(90+377s+162s^2)g'^4$$
$$+ (27+54s+27s^2)g^2\lambda_1 + (9+18s+9s^2)g'^2\lambda_1 - (48+288s-324s^2+624s^3-324s^4)\lambda_1^2\Big)$$
$$+ y_1^2\Big(-\frac{9}{4}g^4 + \frac{21}{2}g^2g'^2 - \frac{19}{4}g'^4 + \lambda_1\big(\frac{45}{2}g^2 + \frac{85}{6}g'^2 + 80g_s^2 - (36+108s^2)\lambda_1\big)\Big)\Big], \tag{A.2d}$$

$$\beta_{y_1} = \frac{y_1}{(4\pi)^2}\left[-\frac{9}{4}g^2 - \frac{17}{12}g'^2 - 8g_s^2 + \left(\frac{23}{6} + \frac{2}{3}s\right)y_1^2\right]$$
$$+ \frac{y_1}{(4\pi)^4}\Big[-\frac{23}{4}g^4 - \frac{3}{4}g^2g'^2 + \frac{1187}{216}g'^4 + 9g^2g_s^2 + \frac{19}{9}g'^2g_s^2 - 108g_s^4$$
$$+ \left(\frac{225}{16}g^2 + \frac{131}{16}g'^2 + 36g_s^2\right)sy_1^2 + 6\left(-2s^2y_1^4 - 2s^3y_1^2\lambda_1 + s^2\lambda_1^2\right)\Big], \tag{A.2e}$$

$$\beta_\xi = \frac{\xi + 1/6}{(4\pi)^2}\left[-\frac{9}{2}g^2 - \frac{3}{2}g'^2 + 6y_1^2 + (6+6s)\lambda_1\right]. \tag{A.2f}$$

Derivation of the beta function β_ξ for the nonminimal coupling ξ is reviewed in [39].

The additional β-functions from the beyond SM sector are given as follows. We do not include s-insertion for these terms as their effects are indirect and negligibly small. We also do not include new particle sector on the running of nonminimal coupling ξ for the same reason.

$$\Delta\beta_{g_s} = \frac{g_s^3}{(4\pi)^2}\frac{2}{3}, \quad \Delta\beta_g = 0, \quad \Delta\beta_{g'} = \frac{g'^3}{(4\pi)^2}\frac{16}{9}, \tag{A.3a}$$

$$\Delta\beta_{\lambda_1} = \frac{1}{(4\pi)^2}\Big(\frac{1}{2}\lambda_3^2 + 12\lambda_1y_2^2 - 6y_2^4 - 12y_1^2y_2^2\Big), \tag{A.3b}$$

$$\Delta\beta_{y_1} = \frac{9}{2(4\pi)^2}y_1y_2^2, \tag{A.3c}$$

$$\beta_{\lambda_2} = \frac{1}{(4\pi)^2}\Big(18\lambda_2^2 + 12y_3^2\lambda_2 + 2\lambda_3^2 - 6y_3^4\Big), \tag{A.3d}$$

$$\beta_{\lambda_3} = \frac{1}{(4\pi)^2}\Big[\lambda_3\big(12\lambda_1 + 6\lambda_2 + 4\lambda_3 + 6y_1^2 + 6y_2^2 + 6y_3^2 - \frac{9}{2}g^2 - \frac{3}{2}g'^2\big) - 12y_2^2y_3^2\Big], \tag{A.3e}$$

$$\beta_{y_2} = \frac{y_2}{(4\pi)^2}\left(\frac{9}{2}y_1^2 + \frac{9}{2}y_2^2 - 8g_s^2 - \frac{9}{4}g^2 - \frac{17}{12}g'^2\right), \tag{A.3f}$$

$$\beta_{y_3} = \frac{y_3}{(4\pi)^2}\left(y_2^2 + \frac{9}{2}y_3^2 - 8g_s^2 - \frac{8}{3}g'^2\right). \tag{A.3g}$$

References

[1] A. A. Starobinsky, Phys. Lett. B **91** (1980) 99.

[2] A. H. Guth, Phys. Rev. D **23** (1981) 347.

[3] K. Sato, Mon. Not. Roy. Astron. Soc. **195** (1981) 467.

[4] A. D. Linde, Phys. Lett. **108**B (1982) 389; Phys. Lett. **129**B (1983) 177.

[5] A. Albrecht and P. J. Steinhardt, Phys. Rev. Lett. **48** (1982) 1220.

[6] P. A. R. Ade, *et al.,* (BICEP2 Collaboration), Phys. Rev. Lett. **112** (2014) 241101 [arXiv:1403.3985v3 [astro-ph.CO]].

[7] P. A. R. Ade, *et al.,* (Planck Collaboration), arXiv:1303.5076 [astro-ph.CO].

[8] P. A. R. Ade, *et al.,* (Planck Collaboration), arXiv:1303.5082 [astro-ph.CO].

[9] H. Liu, P. Mertsch, and S. Sarkar, Astrophys. J. **789** (2014) L29 [arXiv:1404.1899 [astro-ph.CO]].

[10] M. J. Mortonson and U. Seljak, arXiv:1405.5857 [astro-ph.CO]; R. Flauger, J. C. Hill and D. N. Spergel, JCAP **1408** (2014) 039 [arXiv:1405.7351 [astro-ph.CO]].

[11] R. Adam, *et al.,* (Planck Collaboration), arXiv:1409.5738 [astro-ph.CO].

[12] F. L. Bezrukov and M. Shaposhnikov, Phys. Lett. B **659** (2008) 703 [arXiv:0710.3755].

[13] A. O. Barvinsky, A. Y. Kamenshchik, and A. A. Starobinsky, JCAP **0811** (2008) 021 [arXiv:0809.2104]; A. De Simone, M. P. Hertzberg, and F. Wilczek, Phys. Lett. B **678** (2009) 1 [arXiv:0812.4946]; F. L. Bezrukov, A. Magnin, and M. Shaposhnikov, Phys. Lett. B **675** (2009) 88 [arXiv:0812.4950]; C. P. Burgess, H. M. Lee, and M. Trott, JHEP **0909** (2009) 103 [arXiv:0902.4465]; A. O. Barvinsky, A. Y. Kamenshchik, C. Kiefer, A. A. Starobinsky, and C. Steinwachs, JCAP **0912** (2009) 003 [arXiv:0904.1698 [hep-ph]]; A. O. Barvinsky, A. Y. Kamenshchik, C. Kiefer, A. A. Starobinsky, and C. F. Steinwachs, Eur. Phys. J. C **72** (2012) 2219 [arXiv:0910.1041 [hep-ph]]; F. Bezrukov, A. Magnin, M. Shaposhnikov, and S. Sibiryakov, JHEP **1101** (2011) 016 [arXiv:1008.5157]; and references therein.

[14] For a recent review, F. Bezrukov, Class. Quant. Grav. **30** (2013) 214001 [arXiv:1307.0708]; and references therein.

[15] ATLAS and CMS Collaborations, B. Di Micco, "Combinations of Results of Higgs Production in all Decay Channels at LHC", at *XLIX Rencontres de Moriond 2014: QCD and High Energy Interactions,* March 22-29, 2014, Moriond, La Thuile, Italy.
See also the presentations by ATLAS and CMS Collaborations, M. Kado, "Higgs Physics in ATLAS"; A. David, "What CMS Uncovered about the Boson"; at *37th International Conference on High Energy Physics* (ICHEP-2014), Valencia, Spain, July 2-9, 2014.

[16] K. Allison, JHEP **1402** (2014) 040 [arXiv:1306.6931].

[17] The ATLAS, CDF, CMS and D0 Collaborations, arXiv:1403.4427 [hep-ex]; B. Di Micco [ATLAS and CMS Collaborations], "Combinations of Results of Higgs Production in all Decay Channels at LHC", presentation at *XLIX Rencontres de Moriond 2014: QCD and High Energy Interactions*, March 22-29, 2014, Moriond, La Thuile, Italy.

[18] S. Moch, "Precision determination of the top-quark Mass", arXiv:1408.6080 [hep-ph], presentation at the Second Annual Conference on *Large Hadron Collider Physics,* Columbia University, June 2-7, 2014, New York, USA; and references therein.

[19] K. Agashe *et al.,* "Top Quark Working Group Report", arXiv:1311.2028 [hep-ph], Community Summer Study (Snowmass 2013), July 29 – August 6, 2013, Minneapolis, MN, USA.

[20] Y. Hamada, H. Kawai, K. Oda, and S. C. Park, Phys. Rev. Lett. **112** (2014) 241301 [arXiv:1403.5043 [hep-ph]].

[21] F. Bezrukov and M. Shaposhnikov, arXiv:1403.6078 [hep-ph].

[22] Z. Z. Xianyu and H. J. He, JCAP (2014), in Press, [arXiv:1407.6993 [astro-ph.CO]].

[23] J. Ren, Z. Z. Xianyu, H. J. He, JCAP **1406** (2014) 032 [arXiv:1404.4627 [gr-qc]]; Z. Z. Xianyu, J. Ren, H. J. He, Phys. Rev. D **88** (2013) 096013 [arXiv:1305.0251].

[24] C. P. Burgess, S. P. Patil, and M. Trott, JHEP **1406** (2014) 010 [arXiv:1402.1476 [hep-ph]].

[25] A. Spencer-Smith, arXiv:1405.1975 [hep-ph]; A. Kobakhidze and A. Spencer-Smith, arXiv:1404.4709 [hep-ph]; and references therein.

[26] For some recent studies, K. Enqvist, T. Meriniemi, and S. Nurmi, arXiv:1404.3699 [hep-ph]; N. Haba and R. Takahashi, arXiv:1404.4737 [hep-ph]; Y. Hamada, H. Kawai, and K. Oda, arXiv:1404.6141 [hep-ph]; P. Ko and W. I. Park, arXiv:1405.1635 [hep-ph]; N. Haba, H. Ishida, and R. Takahashi, arXiv:1405.5738 [hep-ph]; T. Matsui, arXiv:1405.5700 [hep-ph]; J. Rubio and M. Shaposhnikov, arXiv:1406.5182 [hep-ph]; and references therein.

[27] E.g., R. S. Chivukula, B. A. Dobrescu, H. Georgi, and C. T. Hill, Phys. Rev. D **59** (1999) 075003 [hep-ph/9809470]; H. J. He, C. T. Hill, and T. M. P. Tait, Phys. Rev. D **65** (2002) 055006 [hep-ph/0108041]; H. C. Cheng and J. Gu, arXiv:1406.6689; and references therein.

[28] E.g., S. Dawson and E. Furlan, Phys. Rev. D **86** (2012) 015021 [arXiv:1205.4733]; M. L. Xiao and J. H. Yu, arXiv:1404.0681; S. A. R. Ellis, R. M. Godbole, S. Gopalakrishna, and J. D. Wells, arXiv:1404.4398; and references therein.

[29] J. R. Ellis and D. Ross, Phys. Lett. B **506** (2001) 331 [arXiv:hep-ph/0012067].

[30] Ya. B. Zeldovich, I. Y. Kobzarev, L. B. Okun, Sov. Phys. JETP **40** (1975) 1. For reviews, A. Vilenkin, Phys. Rept. **121** (1985) 263; T. W. B. Kibble, J. Phys. A **9** (1976) 1387; and references therein.

[31] E.g., R. N. Greenwood, D. I. Kaiser, and E. I. Sfakianakis, Phys. Rev. D **87** (2013) 064021 [arXiv:1210.8190].

[32] R. N. Lerner and J. McDonald, Phys. Rev. D **83** (2011) 123522 [arXiv:1104.2468].

[33] F. Bezrukov and M. Shaposhnikov, JHEP **0907** (2009) 089 [arXiv:0904.1537 [hep-ph]].

[34] D. P. George, S. Mooij, and M. Postma, JCAP **1402** (2014) 024 [arXiv:1310.2157].

[35] G. Degrassi, S. Di Vita, J. Elias-Miro, J. Espinosa, G. Giudice, G. Isidori, and A. Strumia, JHEP **1208** (2012) 098 [arXiv:1205.6497].

[36] F. Bezrukov, D. Gorbunov, and M. Shaposhnikov, JCAP **0906** (2009) 029, [arXiv:0812.3622]; J. Garcia-Bellido, D. Figueroa, and J. Rubio, Phys. Rev. D **79** (2009) 063531, [arXiv:0812.4624].

[37] E.g., X. F. Wang, C. Du, H. J. He, Phys. Lett. B **723** (2013) 314 [arXiv:1304.2257]; T. Abe, N. Chen, H. J. He, JHEP **1301** (2013) 082 [arXiv:1207.4103]; J. W. Cui, H. J. He, L. C. Lü, and F. R. Yin, Phys. Rev. D **85** (2012) 096003 [arXiv:1110.6893]; and references therein.

[38] E.g., see presentations at the Kickoff Meeting of Future Circular Collider Study, Feb. 12-15, 2014, Geneva, Switzerland; and the International Workshop on Future High Energy Circular Colliders December 16-17, 2013, IHEP, Beijing, China; M. Bicer *et al.,* [TLEP Working Group],

First Look at the Physics Case of TLEP, JHEP **1401** (2014) 164 [arXiv:1308.6176 [hep-ex]], and references therein.

[39] For reviews, S. D. Odintsov, *Renormalization Group, Effective Action and Grand Unification Theories in Curved Space-time*, Fortsch. Phys. **39** (1991) 621; I. L. Buchbinder, S. D. Odintsov, and I. L. Shapiro, *Effective Action in Quantum Gravity*, published in Bristol, UK, IOP (1992); and references therein.